Passivity Control of a Passive Haptic Device based on Passive FME Analysis

Changhyun Cho[*,**], Beomseop Kim[***,**], Munsang Kim[**], Jae-Bok Song[*], and Mignon Park[***]

[*] Department of Mechanical Engineering, Korea University, Seoul, Korea
(Tel : +82-2-958-6724; E-mail: chcho@kist.re.kr)
[**] Intelligent Robotics Research Center, Korea Institute of Science and Technology (KIST), Seoul, Korea
[***] Department of Electrical and Electronic Engineering, Yonsei University, Seoul, Korea

Abstract: In this paper, a control method is presented to improve performance of haptic display on a passive haptic device equipped with passive actuators. In displaying a virtual wall with the passive haptic device, an unstable behavior occurs with excessive actions of brakes due to the time delay mainly arising from the update rate of the virtual environment and force approximation originated from the characteristics of the passive actuators. The previous T.D.P.C. (Time Domain Passivity Control) method was not suitable for the passive haptic device, since a programmable damper used in the previously introduced T.D.P.C. method easily leads to undesirable behaviors. A new passivity control method is evaluated with considering characteristics of the passive device. First, we propose a control method which is designed under the analysis of the passive FME (Force Manipulability Ellipsoid). And then a passivity control scheme is applied to the proposed control method. Various experiments have been conducted to verify the proposed method with a 2-link mechanism.

Keywords: Passive haptic device, FME, force approximation, and passivity

1. INTRODUCTION

As generally known, a passive actuator such as a brake is stable and has an advantage of a good torque/mass ratio. Furthermore, its relatively small energy consumption makes it suitable for portable devices. Since most real or virtual environments can be modeled as passive systems, use of passive actuators for haptic devices can be justified. Taking all these benefits into account, passive haptic devices equipped with passive actuators can be a good solution to portable or wearable haptic devices. The most serious drawback of passive haptic devices is that passive actuators can generate a torque only against rotation of its shaft. Needless to say, passive actuators cannot produce energy but dissipate it. This feature is beneficial in the light of stability, but it often leads to poor performance in haptic display in that passive actuators are not able to generate a torque in arbitrary directions.

Planar passive haptic devices have been evaluated. Book et al. presented a planar haptic device based on the 5-bar mechanism equipped with four brakes for 2 DOF haptic display [1]. This redundancy in actuation increased haptic performance of the device. As a successive research, Swanson and Book presented the single degree of freedom controller (SDOF Controller), which used SDOF line achieved by locking one brake to reduce system's DOF [2]. To avoid the unsmooth display, Swanson and Book also presented an optimal control concept on the proposed velocity ratio controller which was applied on a velocity field [3]. Cost functions were constructed to minimize approximation angle and kinetic energy loss. However, a velocity filed should be determined before displaying a desired path.

Sakaguchi et al. presented the passive haptic device with 5 bar mechanism and two ER (Electro-Rheological) brakes [4]. To move along the surface of a virtual wall, a small band was set up near the surface. Only one brake was activated in the small band as in the SDOF controller in [2]. However, the proposed method for moving along the surface could disturb motion toward the free space.

Most researches on a passive haptic device were mainly focused on coping with the problems related to passive haptic devices such as force approximation, which is generally known as a cause of unsmooth motion. In case of an active haptic device, control schemes for wall contact and wall following are consistent with each other. It just displays a desired force which prevents penetration into the virtual wall in the wall contact and guides the device along the wall surface in the wall following. This feature should be applied to a passive haptic system. Thus in this paper we will focus on developing a consistent control method, which only displays a desired force, for overcoming the limitation arisen from the time delay and force approximation.

Cho et al. [5] proposed the analysis method of a passive haptic device using the passive FME (Force Manipulability Ellipsoid), which graphically illustrates the mapping between a torque in joint space and a force in task space [6]. The time delay and force approximation lead to an active behavior like as an active haptic device even in a passive haptic device. The T.D.P.C. (Time Domain Passivity Control) method evaluated for an active haptic device is adopted into a passive haptic device (or system) for solving the unstable behavior (i.e., unsmooth motion) [7]. However, the T.D.P.C. method is not suitable for a passive haptic device, since it easily leads to undesirable behaviors such as retarding motion along a surface of a frictionless virtual wall caused by not only a passive actuator but also the T.D.P.C. method. A new T.D.P.C. method for a passive haptic device can be evaluated with using the passive FME. The force distribution at the end-effector can be readily available by using the passive FME, which leads to a control scheme. It multiplies a desired force by a scale factor to avoid the excessive actions of brakes. And then we design a new energy based control method which calculates the scale factor of the control scheme evaluated form the passive FME with passivity ideas.

The rest of this paper is organized as follows. The passive FME is briefly introduced in Section 2, and limitations of the previous T.D.P.C. method are investigated with application to a passive haptic device in Section 3. A new force control scheme is proposed in Section 4. Section 5 deals with the 2 DOF coupled tendon-drive mechanism which was developed for experimental verification of the proposed control method and shows some experimental results. Conclusions are drawn in Section 6.

2. PASSIVE FME

It is generally known that a passive actuator can generate a torque only against rotation of its shaft. From this well known fact, constraint equations based on the Karnopp's stick-slip

model can be acquired with considering haptic display [8].

Slip mode ($\dot{\theta} \neq 0$)

$$\tau_c = \begin{cases} -\text{sgn}(\dot{\theta})|\tau_d| & \text{if } \text{sgn}(\dot{\theta}) \neq \text{sgn}(\tau_d) \\ 0 & \text{else} \end{cases} \quad (1a)$$

Stick mode ($\dot{\theta} = 0$)

$$\tau_c = \begin{cases} -\tau_h & \text{if } \text{sgn}(\tau_h) \neq \text{sgn}(\tau_d) \\ 0 & \text{else} \end{cases} \quad (1b)$$

where τ_d is the desired torque required for haptic display (i.e., force reflection) and τ_h is the hand torque input to the device by a human operator. And $\dot{\theta}$ is the joint velocity, and τ_c is the control torque generated by the brake. The control torque is created in the direction opposite to either its shaft rotation in Eq. (1a) or the external hand torque acting on its shaft in Eq. (1b). Note that if a desired torque has the same sign as a joint velocity or a hand torque, the brake should be released (i.e., $\tau_c = 0$) to avoid producing a brake torque which is against the user's intention. In this paper Eq. (1) will be termed as the passive constraint.

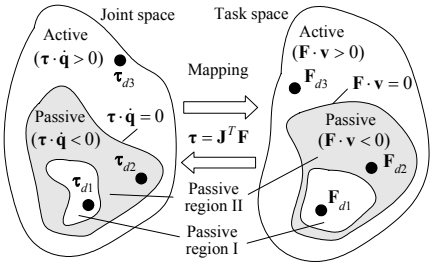

Fig. 1 Mapping between joint and task spaces.

To investigate limitations of a passive haptic device, consider the Jacobian mapping between the joint torque in joint space and the end-effector force in task space as shown in Fig. 1. The inner product of the torque vector and the angular velocity vector for the n DOF mechanism is given by

$$\boldsymbol{\tau}\cdot\dot{\mathbf{q}} = \sum_{i=1}^{n} \tau_i \cdot \dot{q}_i \quad (2)$$

The joint space can be divided into the active region where $\boldsymbol{\tau}\cdot\dot{\mathbf{q}} > 0$ and the passive region where $\boldsymbol{\tau}\cdot\dot{\mathbf{q}} \le 0$. The passive region is further divided into passive region I in which all joints satisfy the passive constraint (i.e., $\tau_i \cdot \dot{q}_i \le 0$ for all i) and passive region II in which not all joints satisfy the passive constraint (i.e., $\tau_i \cdot \dot{q}_i > 0$ for some i). Brakes, therefore, can generate a brake torque only in passive region I. Note that motors can create any torque in the entire joint space. Passive region I in joint space is mapped into the corresponding passive region I in task space, but its distribution or shape in task space cannot be easily estimated from the information on the joint space. In what follows, a method for representing passive region I in task space will be described by the Jacobian mapping:

$$\boldsymbol{\tau} = \mathbf{J}(\mathbf{q})^T \mathbf{F} \quad (3)$$

where $\mathbf{J}$ is the manipulator Jacobian matrix, $\mathbf{q}$ is the n-dimensional joint variable vector, and $\mathbf{F}$ is the m-dimensional end-effector force vector, respectively. A so-called force manipulability ellipsoid (FME) can be drawn from Eq. (3) by finding a set of all end-effector forces that are realizable by a joint torque vector whose Euclidean norm satisfies the condition $\|\boldsymbol{\tau}\| = (\tau_1^2 + \cdots + \tau_n^2)^{1/2} \le 1$.

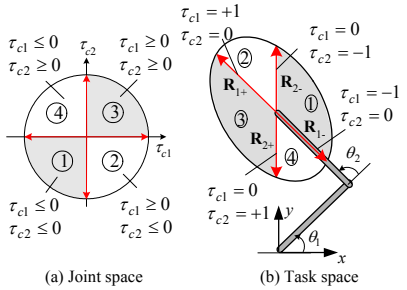

Fig. 2 A set of passive FMEs ($\theta_1 = 45^o$, $\theta_2 = 90^o$, $l_1 = l_2 = l$).

Possible sets of joint torque can be acquired by Eq. (1) as shown in Fig. 2(a). Thus each region in Fig. 2(a) represents the passive region I in the joint space and is then mapped into the corresponding region in task space by Eq. (3) as illustrated in Fig. 2(b). In passive haptic devices, the joint torque is closely related to the joint velocity by the passive constraint given by Eq. (1). Referring to Eq. (1), for example, only joint torques of $\tau_{c1} \le 0$ and $\tau_{c2} \le 0$ are available in region 1, if $\dot{\theta}_1 > 0$ and $\dot{\theta}_2 > 0$. When $\dot{\theta}_1 > 0$ and $\dot{\theta}_2 = 0$, for instance, $\tau_{c1} \le 0$ but τ_{c2} is determined only by τ_{h2} (see Eq. (1b)). From all possible combinations of joint velocities, we observed that control torques can be represented by 4 regions in Fig. 2(a) regardless of whether the joints are in either the slip mode or the stick mode.

A set of passive FMEs can be drawn by mapping $\boldsymbol{\tau}_c$ in joint space into the end-effector force $\mathbf{F}_c$ in task space using the Jacobian mapping of Eq. (3). Thus each region in Fig. 2(a) is mapped into each corresponding passive FME illustrated in Fig. 2(b) which represents a set of passive FMEs. Each passive FME is delimited by four reference forces $\mathbf{R}_{1+}$, $\mathbf{R}_{1-}$, $\mathbf{R}_{2+}$, and $\mathbf{R}_{2-}$, where $\mathbf{R}_i$ denotes the end-effector force when only brake i is applied (i.e., $\tau_{ci} \neq 0$) with the other brakes released. For example, if $\tau_{c1} > 0$ (or $\tau_{c1} < 0$) with $\tau_{c2} = 0$, then force $\mathbf{R}_{1+}$ (or $\mathbf{R}_{1-}$) is generated. Likewise, $\mathbf{R}_{2+}$ (or $\mathbf{R}_{2-}$) is generated for $\tau_{c2} > 0$ (or $\tau_{c2} < 0$) with $\tau_{c1} = 0$. Note that the Jacobian and thus reference forces change as the manipulator moves.

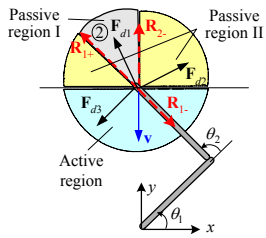

Fig. 3. Force approximation ($\theta_1 = 45^o$, $\theta_2 = 90^o$, $l_1 = l_2 = l$).

Consider an example in Fig. 3 for detailed analysis. Suppose that the end-effector P is moving in the $-y$ direction, in which $\dot{\theta}_1 < 0$ and $\dot{\theta}_2 > 0$. Hence, the brakes can generate a force only in passive FME 2 (i.e., $\tau_{c1} > 0$ and $\tau_{c2} < 0$) because of the passive constraint. Note in passive FME 2 that $\tau_{c1}\dot{\theta}_1 < 0$ and $\tau_{c2}\dot{\theta}_2 < 0$, and thus $\boldsymbol{\tau}\cdot\dot{\mathbf{q}} = \tau_{c1}\dot{\theta}_1 + \tau_{c2}\dot{\theta}_2 < 0$ in Eq. (2). Since passive FME 2 belongs to passive region I, the desired force $\mathbf{F}_{d1}$ in this region can be accurately displayed by a resultant force of $\mathbf{R}_{1+}$ and $\mathbf{R}_{2-}$. On the other hand, the

desired $\mathbf{F}_{d2}$ belonging to passive region II needs to be represented by a combined force of $\mathbf{R}_{2-}$ and $\mathbf{R}_{1-}$ in Fig. 2, but generation of $\mathbf{R}_{1-}$ requires $\tau_{c1} < 0$ which violates the passive constraint of $\tau_{c1} \cdot \dot{\theta}_1 \le 0$. Therefore, $\mathbf{F}_{d2}$ cannot be accurately displayed but only approximately by the nearest available force $\mathbf{R}_{2-}$ alone, which will be called 'force approximation' in passive haptic devices. Finally, the desired force $\mathbf{F}_{d3}$ cannot be displayed at all since it belongs to the active region of $\mathbf{F} \cdot \mathbf{V} > 0$. Consequently, there exist regions in which the desired force cannot be displayed or can be displayed only approximately in the case of passive haptic devices, and these regions can be found by the passive FME analysis.

3. THE PREVIOUS T.D.P.C. METHOD

So called the T.D.P.C (Time Domain Passivity Control) method proposed by Hannaford and Ryu has great merits in its implementation and robustness, since it does not use any system information (e.g., a dynamic model of a haptic device) [7,9]. Moreover, a passive haptic device is a non-linear system, which leads to a complicated dynamic model. Taking this complicity of model into account, use of the T.D.P.C. method can be justified in practical point of view.

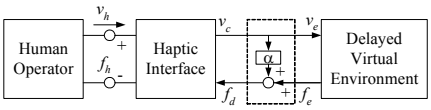

Fig. 4 Basic haptic interface system with delayed virtual environment [7].

In haptic display, a function of the T.D.P.C. method is to operate a programmable damper between the virtual environment and the haptic device. That is, if excessive energy is occurred, T.D.P.C. method makes the system stable using the programmable damper. So the T.D.P.C. consists of PO (Passivity Observer) which measures the system energy and PC (Passivity Controller) which activates programmable damper. Fig. 4 is a block diagram about haptic system with time delayed virtual environment, where v_h is the input speed to the end-effector and v_e is that of the virtual environment. f_h (or f_e) is the acting force to haptic device (or the desired force from the virtual environment), and v_c is the output velocity from haptic device. f_d is the control force calculated by PC. And the passivity is defined as follow.

$$P = \int_0^t f(\tau)v(\tau)d\tau + E(0) \tag{4}$$

where $E(0)$ is an initial energy. If the sign of Eq. (4) is negative, the system is active, and in the other case that is passive. The programmable damper by PC should be attached in the direction of a desired force. Thus every v_c and v_e in Fig. 4 should be components of velocity in the direction of the desired force [10]. According to the series PC, the definition of control force f_d for a haptic device is as follows.

$$f_d = f_e + \alpha v \tag{5}$$

where, $v_e = v_c = v$. Eq. (5) denotes adding virtual damping force to a desired force f_e. PO for a time delayed virtual environment is as follows.

$$W(k) = \sum_{k=1}^{n} f_d(k-1)v(k)\Delta t + W_0 \tag{6}$$

where Δt is a sampling period and W_0 is initial passivity. Eq. (6) represents the passivity at n_{th} instant. A prediction of the passivity for $(n+1)_{th}$ instant at n_{th} instant can be drawn as follow.

$$W_c(k+1) = W(k) + f_e(k)v(k)\Delta t \tag{7}$$

If Eq. (7) < 0 or less than any value which can be absorbed by a haptic device, the observed system is active. α is calculated for stabilizing the system. For simplicity, absorbed passivity by a haptic device is neglected in this paper. The following is an equation for calculating α.

$$\alpha(k) = -W_c(k+1)/v_e(k)^2 \quad \text{If } W_c(k) < 0 \tag{8}$$

Hereby α has always positive sign. Eq. (8) shows the way to calculating damping coefficient which can wholly dissipate the stored energy at that instant.

In passive haptic device, the PC affects over damping effect, since controlling brake is conducted by the passive constraint defined in Section 2. For easy understanding, we suppose simple 1 DOF haptic display and assume that $W(n) < 0$ for activating PC (see Eq. (8)). Suppose that the direction of velocity toward outside of the wall is positive. If the end-effector penetrates a virtual wall, $f_e < 0$ for all instant (remind that the system is active in the point of view of the passivity idea, when the passivity (i.e., Eq. (4) or (6)) is less than zero.). In case that operator intends to pull the end-effector out toward outside the wall (i.e., $v > 0$), conditions of f_e and αv are as follows: $|f_e| < |\alpha v|$, $|f_e| = |\alpha v|$, and $|f_e| > |\alpha v|$. In each case we calculate f_d by Eq. (5): $f_d > 0$, $f_d = 0$, and $f_d < 0$. In case of $f_d = 0$, desired force is set to zero. Therefore a brake is fully released in spite of the penetration inside the wall. Also in case of $f_d < 0$, product of force and velocity is $f_d \cdot v < 0$. So f_d is the force in active region and a brake is fully released due to the passive constraint. A product of force and velocity is $f_e \cdot v < 0$ (i.e., active region, all brake must be released.). Thus the operator can pull out the end-effector without feeling any retarding force. However, in case of $f_d > 0$, f_d has the opposite sign of f_e and product of force and velocity is $f_d \cdot v > 0$. So f_d is the force in Passive region I and brake will be activated (see Eq. (1a)). Considering the direction of f_d, it is opposite to the operator's intention. Thus changing the sign of desired force f_d leads to a retarding force against the operator's intention and this situation is not desirable.

4. T.D.P.C. FOR A PASSIVE HAPTIC DEVICE

4.1 Direct control method

Fig. 5 illustrates various forces involved in representing a virtual wall. A proper brake control scheme can be found by observing the relations of these forces. **n** and **t** are a surface normal and tangent vector of the wall respectably. If a desired force $\mathbf{F}_d$ is displayed approximately by the reference force $\mathbf{R}_{2+}$, for example, then the control force $\mathbf{F}_c$ is generated by the brake in the direction of $\mathbf{R}_{2+}$. $\mathbf{F}_h$ is a hand force input by user and $\mathbf{F}_{hc}$ and $\mathbf{F}_{hct}$ are its components parallel and perpendicular to $\mathbf{F}_c$. $\mathbf{F}_h$ is assumed to be constant for easy understanding. An angle between $\mathbf{F}_d$ and $\mathbf{F}_c$ can be termed as an approximation angle, which will represent a level of the force approximation. The greater approximation angle leads to the poorer haptic display in a passive haptic device. The resultant $\mathbf{F}_r$ of all the forces acting on the end-effector becomes

$$\begin{aligned} \mathbf{F}_r &= \mathbf{F}_{rn} + \mathbf{F}_{rt} \\ &= \mathbf{F}_{hc} + \mathbf{F}_{hct} + \alpha \mathbf{F}_c \\ &= \mathbf{F}_h + \alpha \mathbf{F}_c \end{aligned} \tag{9}$$

where $\mathbf{F}_{rt}$ and $\mathbf{F}_{rn}$ are the tangent and normal components of $\mathbf{F}_r$, and α is the scale factor to be determined. Equation 8 satisfies the both slip and stick mode. Suppose that $|\mathbf{F}_{hc}| \le |\alpha\mathbf{F}_c|$. Brake 2 is in the stick mode ($|\alpha\mathbf{F}_c| = |-\mathbf{F}_{hc}|$). So $\mathbf{F}_{hc}$ is canceled out with $\mathbf{F}_c$ and only $\mathbf{F}_{hct}$ remains in $\mathbf{F}_r$. In case of the slip mode ($|\mathbf{F}_{hc}| > |\alpha\mathbf{F}_c|$), a force in $\mathbf{F}_c$ direction will be $\mathbf{F}_{hc} + \alpha\mathbf{F}_c$. Thus Eq. (9) holds for all cases. From the observation that unsmooth wall following is caused by repeated contact and non-contact of the end-effector with the wall, the proposed brake control attempts to make the normal component $\mathbf{F}_{rn}$ be zero by adjustment of a brake torque. Then the end-effector becomes subject to only the tangential force along the surface, thereby leading to smooth wall following without leaving the wall surface. In what follows, the scale factor which makes $\mathbf{F}_{rn}$ vanish will be derived.

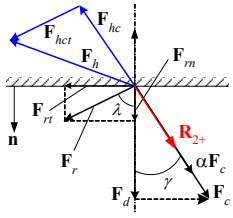

Fig. 5 Forces acting on the end-effector.

First, $|\mathbf{F}_{rn}|$ is computed by

$$|\mathbf{F}_{rn}| = |\mathbf{F}_r| \cos\lambda \tag{10}$$

where λ is the angle included between $\mathbf{F}_d$ and $\mathbf{F}_r$. Since the desired force $\mathbf{F}_d$ is normal to the surface, and thus $\mathbf{n} = \mathbf{F}_d / |\mathbf{F}_d|$, $\cos\lambda$ can be expressed by

$$\cos\lambda = \mathbf{F}_r \cdot \mathbf{F}_d / (|\mathbf{F}_r||\mathbf{F}_d|) \tag{11}$$

Substitution of Eq. (9) and Eq. (11) into Eq. (10) yields

$$|\mathbf{F}_{rn}| = |\mathbf{F}_h + \alpha\mathbf{F}_c| ((\mathbf{F}_h + \alpha\mathbf{F}_c) \cdot \mathbf{F}_d) / (|\mathbf{F}_r||\mathbf{F}_d|) \tag{12}$$

Because $\mathbf{F}_r = \mathbf{F}_h + \alpha\mathbf{F}_c \neq 0$ in general, $|\mathbf{F}_{rn}| = 0$ can be achieved when

$$(\mathbf{F}_h + \alpha\mathbf{F}_c) \cdot \mathbf{F}_d = 0 \tag{13}$$

Hence, α can be obtained by

$$\alpha = -(\mathbf{F}_h \cdot \mathbf{F}_d) / (\mathbf{F}_c \cdot \mathbf{F}_d) \tag{14}$$

Let us investigate the sign of α. Only when $\mathbf{F}_h \cdot \mathbf{F}_d < 0$, the user intends to move the end-effector while maintaining it in contact with the wall; otherwise, the user intends to move the end-effector off the wall and thus force reflection is not necessary. On the other hand, only when $\mathbf{F}_c \cdot \mathbf{F}_d > 0$, the approximation angle γ between the desired and the reference force is less than 90° and thus force approximation is possible. Consequently, $\alpha > 0$ since $\mathbf{F}_h \cdot \mathbf{F}_d < 0$ and $\mathbf{F}_c \cdot \mathbf{F}_d > 0$. Furthermore, the value of α is in the range of $0 < \alpha \le 1$. Note that $\alpha > 1$ means that the brake is commanded to generate the torque greater than the desired torque, which is unreasonable.

Considering that a virtual wall generally has the bilateral characteristic, it is appropriate that α should be computed by Eq. (14) while the end-effector is inside the wall but moves outwardly. The outward motion can cause the unstable behavior as like that of an active haptic device. When the end-effector moves inwardly, brakes are firmly activated to retard the on-going penetration of the end-effector. Thus, α should be computed with Eq. (14), when $\mathbf{F}_d \cdot \mathbf{v} > 0$ (i.e., outward motion). This proposed scheme is called direct control scheme because the value of α can be determined directly from the passive FME. The direct controller is implemented as follows:

1. Compute the control force $\mathbf{F}_c$ depending on $\mathbf{F}_d$.
2. $\alpha = \begin{cases} -(\mathbf{F}_h \cdot \mathbf{F}_d)/(\mathbf{F}_c \cdot \mathbf{F}_d) & \text{if } \mathbf{F}_d \cdot \mathbf{v} > 0 \\ 1 & \text{else} \end{cases}$
3. Set $\mathbf{F}_c' = \alpha\mathbf{F}_c$
4. Generate brake torques according to $\boldsymbol{\tau}_c' = \mathbf{J}^T \mathbf{F}_c'$.

Note that if $\mathbf{F}_d$ is in passive region I, then $\mathbf{F}_c$ is set to $\mathbf{F}_d$, whereas if in passive region II, then $\mathbf{F}_c$ is selected so that its component in the normal direction becomes $\mathbf{F}_d$.

4.2 Indirect control method

Measuring noises of $\mathbf{F}_h$ can seriously degrade performance of the direct control method. An expensive F/T (Force/Torque) sensor is needed for measuring $\mathbf{F}_h$ precisely. For practical implementation it is not desirable and therefore a control scheme without any high precision F/T sensor is needed. An energy-based approach will be adopted for building a new control scheme that α of direct control method is calculated with passivity ideas.

The unstable behavior of passive haptic device is caused by time delay and force approximation, so PO should contain these active factors. Haptic interface of passive haptic device is shown in Fig. 6. Time delay is mainly caused by update rates of a virtual environment, and force approximation occurs due to the limitation of a passive haptic device. So the passivity in the dotted area in Fig. 6 should be considered.

$$W_{pc} = vf_{c2} - vf_{c1} \tag{15}$$

$$W_{hc} = vf_{c1} - vf_e \tag{16}$$

$$W_{ve} = vf_e \tag{17}$$

Eq. (15), (16) and (17) denote change rate of passivity of each elements such as passivity controller (PC), passive constraint and virtual environment respectively. By adding all equations, change rate of passivity of the boxed area can be calculated and then passivity of the area can be computed by integrating it. A discrete form of passivity of the area can be represented as follow.

$$W(k) = \sum_{k=1}^{n} v(k) f_{c2}(k-1)\Delta t + W_0 \tag{18}$$

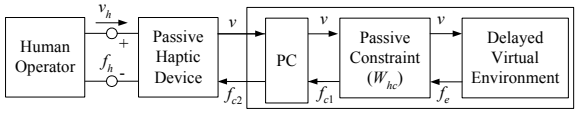

Fig. 6 Haptic interface system of a passive haptic device with delayed virtual environment.

A new control method using passivity ideas is originated form the direct method. α in the direct control method is calculated to avoid excessive force reflection for guaranteeing stability of a passive haptic device. In a new control method α will be calculated by the energy-based approach. Thus f_{c2} can have the same form as that of the direct (see step (3) of implementation of the direct).

$$f_{c2} = \alpha f_{c1} \tag{19}$$

With Eq. (19), Eq. (18) can be represented as follows.

$$W(k) = \sum_{k=1}^{n} \alpha(k-1) f_{c1}(k-1) v(k) \Delta t + W_0 \quad (20)$$

Equation (20) denotes passivity at instant k. A predicted energy for instant k+1 at instant k is as follows.

$$W_c(k+1) = W(k) + v(k) f_{c1}(k) \Delta t \quad (21)$$

$\alpha(k)$ also have the same bound ($0 < \alpha \le 1$) as that of the direct. Considering Eq. (19), α can be calculated using change rate of passivity. A change rate of passivity is defined as follows.

$$\alpha(k) v(k) f_{c1}(k) = \kappa \quad (22)$$

where κ is a constant. If κ is set to a fixed constant for all time, the adaptability of the control method can be degraded. Suppose that passivity has quite large negative value (i.e., very unstable). κ should be rapidly set to very small value which makes the system stable. Thus κ can be described in inverse proportion to passivity as follows.

$$\kappa = K / W_c \quad (23)$$

where, K is an arbitrary constant. In Eq. (22) and (23) $\alpha(k)$ is calculated as follows.

$$\alpha(k) = \begin{cases} K/(v(k) f_{c1}(k) W_c) & \text{if } W_c < 0,\ v(k) f_{c1}(k) < 0 \\ 1 & \text{else} \end{cases} \quad (24)$$

Since α is calculated indirectly by passivity like as Eq. (24), this energy-based method can be termed as the indirect control method. Implementation of the indirect control method is as follows.

1. Calculating f_{c1} by passive constraint
2. Computing passivity and predicted passivity (Eq. (20) and (21)).
3. $\alpha(k) = \begin{cases} K/(v(k) f_{c1}(k) W_c) & \text{if } W_c < 0,\ v(k) f_{c1}(k) < 0 \\ 1 & \text{else} \end{cases}$
4. Set $f_{c2} = \alpha f_{c1}$
5. Generate brake torques

5. EXPERIMENTS

5.1 Experimental setup

The 2-link passive haptic device equipped with 2 electric brakes shown in Fig. 7 was constructed for experiments. The angles θ_i and θ_{Bi} represent the joint angle and the rotating angle of the brake, respectively, and k_i is the reduction ratio of the tendon-drive system. Brake 1 (or 2), which provides a braking torque to link 1 (or 2), is mounted at the base and conveys the torque through pulleys P_{1a}-P_{1b} (or P_{2a}-P_{2b}). Placing both brakes at the base has an advantage of reducing the mass of the moving part. The FT (force/torque) sensor is mounted at the handle to measure the hand force provided by the user. The directions of exerting hand torques are calculated with the measured hand force input by using Eq. (3) so to draw a passive FME even though a joint velocity is zero (i.e., the stick mode). Rotational motion of each brake is sensed by the optical encoder mounted on the brake axis.

In the experiments, the brake control is conducted at a rate of 1kHz, and the response time of the brake is about 20ms. Since the brake is capable of generating a braking torque proportional to the current input, it is controlled in an open-loop manner. The virtual wall is modeled as a spring whose constant is 10^7N/m, but is assumed to possess neither damping nor friction on the surface. Thus the direction of a desired force is in that of the surface normal **n**.

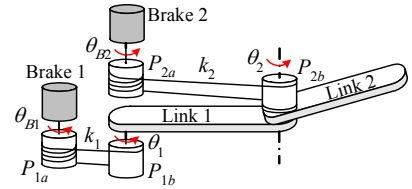

(a) Schematic

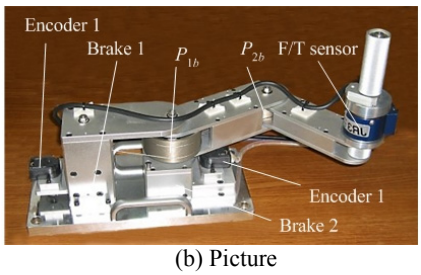

(b) Picture

Fig. 7 Coupled tendon-drive mechanism.

5.2 Experimental results

Experimental Results in Fig. 8 are for a plain virtual wall whose surface normal is directed to $-y$ direction and offset form the origin is 0.225m. A hand force input is provided by the human operator to move the handle mounted at the end-effector in $+x$ direction with maintaining contact with the virtual wall. In this situation the force approximation occurs and $\mathbf{R}_2$- is used for displaying the virtual (in the special configuration that $\theta_2 < 0^o$). Thus only brake 2 is activated and brake 1 is fully released during the display of the virtual wall and thus directions of control forces are coincided with those of $\mathbf{R}_2$-. The approximation angle γ, which is an angle between a desired force and control force as shown in Fig. 5, increase, as the end-effector is moved in $+x$ direction. The min and max approximation angles are 3^o around x = 0.06m and 33^o around x = 0.17m. For practical implementation of the direct and indirect control, the maximum difference of α in Eq. (14) and (24) within the control period of brake is set to some reasonable value (in this case, 0.01) so to avoid oscillations of α due to the noises on joint velocities.

The result in Fig. 8 is conducted at 50Hz update rates of the virtual wall. It is shown that excessive penetration into the wall occurs initially around x = 0.06m, although the spring constant of the virtual wall is large (i.e., 10^7N/m). This is caused by the time delay due to rather dynamic characteristic of the brake than slow update of the virtual wall. It is closely related to the response time of the brake and velocity at contact. Using brakes, which have faster response time, or slower velocity at contact will reduce the penetration depth. Thus it is not great concern. There shows a smooth path of the end-effector after the first contact in case of the direct and indirect control. However, that of no control is illustrated with contact and non-contact behaviors (i.e., A - D points in Fig. 8).

Comparing the tendency of the velocity of brake 2 (i.e., ω_{B2}) for the direct and indirect control with that of no control, 'Stick2' does not appear in case of the direct and indirect control. This means that brake 2 is not completely locked on the pullback situation in case of the direct and indirect control, which is intended by the proposed controls. The scale factor α calculated by Eq. (14) or (24) is nearly zero for compensating the very large desired forces ($5\text{x}10^4$ N) with the small hand

force inputs (below 3N, F_{hy} in Fig. 8). Abrupt changes of F_{hy} are greatly reduced in the direct control, whereas those of no control vary abruptly with large amplitude. Thus the tendency of F_{hy} can also say that the smooth motion is provided by the proposed control methods. However, F_{hx} increase as the approximation angle γ increases. It means that the human operator feels stronger force, which retards the motion along the surface as like a friction force, as the approximation angle increases. This can be easily understood with investigating forces acting on the end-effector shown in Fig. 5. In Fig. 5, there exists an undesired force due to the force approximation in the tangent direction, which can be calculated as $|\alpha\mathbf{F}_c|\sin(\gamma)$. Thus the undesired force increases as the approximation angle increases within 0~90° range (in this experiments, $3^o \le \gamma \le 33^o$). During controlling brake 2, F_{hx} of the proposed control methods are less than that of the no control, since a retarding force in case of the no control (i.e., $|\mathbf{F}_c|\sin(\gamma)$) is greater than that of the direct control (i.e., $|\alpha\mathbf{F}_c|\sin(\gamma)$). It is so natural, because $|\mathbf{F}_c| > |\alpha\mathbf{F}_c|$ ($0 < \alpha \le 1$). Thus it can be drawn that the human operator feels less retarding force along the surface with the proposed control.

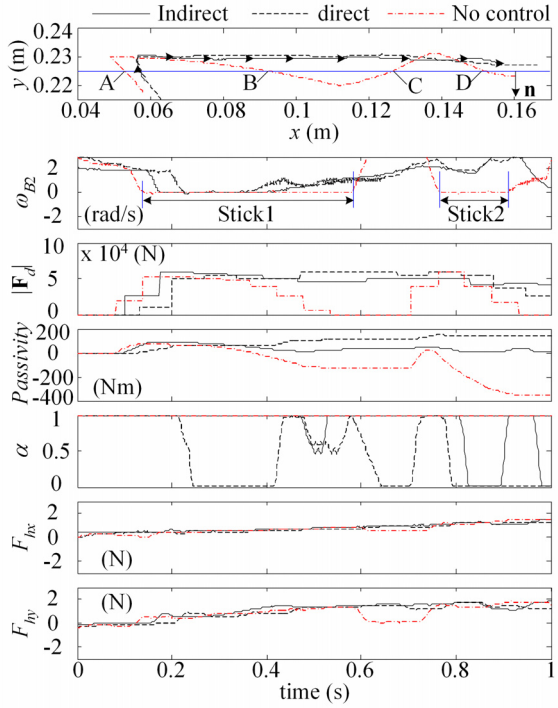

Fig. 8 Experimental results on a plain wall with 20Hz update rates of the virtual wall.

Both the direct and indirect control show similar performance on the wall following task form the above observation. However, energy behaviors (i.e., 'Passivity' in Fig. 8) are quiet different. The no control shows an unstable behavior (i.e., passivity < 0), whereas both the proposed methods show stable behaviors for all time in sense of the passivity ideas. In case of the direct control method passivity increases as time goes, whereas it converges on a positive constant value in case of the indirect control method. One may have any curiosity on calculating α with the indirect method. Why the adaptation occurs on the stable situation? Referring to Eq. (24), α is calculated, when not actual passivity $W < 0$ but estimated passivity $W_c < 0$. The passivity shown in Fig. 8 is for the actual one. It is noted that the indirect method does not use any high precision F/T sensor as like the direct method. It only requires signs of exerting torques at joints or brakes for determining the reference force which is used in force approximation.

6. CONCLUSION

In this research, two control methods are proposed to solve the problems with passive haptic devices due to force approximation and time delay. From analyses and various experiments, the following conclusions are drawn:

1. An undesired force due to force approximation retards motion of the end-effector along the surface.
2. The retarding force increases as the approximation angle increase within 0~90° range.
3. Less retarding forces are produced by the proposed control methods.
4. The proposed control methods can improve performance of wall following task with a passive haptic device regardless of time delay.
5. In case of the direct method, passivity always increases during contact, which means that it leads to an excessively stable behavior. However, in case of the indirect method, passivity is maintained around zero during contact.

We observed the performance degradation due to the noise in velocity. A robust design of the indirect method on the noise is required for practical implementation.

REFERENCES

[1] W. J. Book, R. Charles, H. Davis, and M. Gomes, "The concept and implementation of a passive trajectory enhancing robot," Proc. of the ASME Dynamic Systems and Control Division, pp.633-638, 1996

[2] D. K. Swanson and W. J. Book, "Obstacle avoidance methods for a passive haptic display," Proc. of the IEEE Int. Conf. on Advanced Intelligent Mechatronics, pp.1187-1192, 2001.

[3] D. K. Swanson and W. J. Book, "Path-following control for dissipative passive haptic displays," Proc. of 11th Symposium on Haptics, pp. 101-108, 2003.

[4] M. Sakaguchi, J. Furusho and N. Takesue, "Passive force display using ER brakes and its control experiments," Proc. of Virtual Reality, pp.7-12, 2001.

[5] C. H. Cho, M. S. Kim and J. B. Song, "Performance analysis of a 2-link haptic device with electric brakes," Proc. of 11th Symposium on Haptics, pp. 47 -53, 2003.

[6] T. Yoshikawa, Foundations of Robotics: Analysis and Control, The MIT Press, 1990.

[7] B. Hannaford and J. H. Ryu, "Time domain Passivity Control of Haptic Interfaces," IEEE Trans. On Robotics and Automation, vol. 18, No. 1, pp. 1-10, 2002.

[8] D. Karnopp, "Computer simulation of stick-slip friction in mechanical dynamic system," ASME Journal of Dynamic Systems, Measurement, and Control, vol. 107, pp.100-103. 1985.

[9] J. H. Ryu, Y. S. Kim, and B. Hannaford, "Sampled and Continuous Time Passivity and Stability of Virtual Environments," Proc. of the IEEE Int. Conf. on Robotics and Automation, 2003, to be published.

[10] C. Preusche, G. Hirzinger, J. H. Ryu, and B. Hannaford, "Time Domain Passivity Control for 6 Degrees of Freedom Haptic Displays," Proc. of the IEEE/RJS Int. Conf. on Intelligent Robotics and systems, 2003, to be published.